

Subatmospheric Vapor Pressures Evaluated from Internal-Energy Measurements

H. A. Duarte-Garza^{1,2} and J. W. Magee^{1,3}

Received May 30, 1996

Vapor pressures were evaluated from measured internal-energy changes in the vapor + liquid two-phase region, $\Delta U^{(2)}$. The method employed a thermodynamic relationship between the derivative quantity $(\partial U^{(2)}/\partial T)_p$ and the vapor pressure (p_σ) and its temperature derivative $(\partial p_\sigma/\partial T)_\sigma$. This method was applied at temperatures between the triple point and the normal boiling point of three substances: 1,1,1,2-tetrafluoroethane (R134a), pentafluoroethane (R125), and difluoromethane (R32). Agreement with experimentally measured vapor pressures near the normal boiling point (101.325 kPa) was within the experimental uncertainty of approximately ± 0.04 kPa ($\pm 0.04\%$). The method was applied to R134a to test the thermodynamic consistency of a published p - p_σ - T equation of state with an equation for p_σ for this substance. It was also applied to evaluate published p_σ data which are in disagreement by more than their claimed uncertainty.

KEY WORDS: difluoromethane; internal energy; pentafluoroethane; refrigerants; 1,1,1,2-tetrafluoroethane; triple point; two-phase region; vapor pressure.

1. INTRODUCTION

Ambrose and Davies [1] have reviewed developments in measurement and estimation of low-pressure vapor pressures below the atmospheric range of 1 to 200 kPa. They have concluded that most of the methods for the measurement of low-pressure values are time-consuming and relatively inaccurate, and improved methods need to be developed. For these reasons, we seek to develop better estimation procedures which may extrapolate high-accuracy vapor pressures in the atmospheric range

¹ Physical and Chemical Properties Division, Chemical Science and Technology Laboratory, National Institute of Standards and Technology, Boulder, Colorado 80303, U.S.A.

² Guest researcher from Texas A&M University, Kingsville, Texas 78363, U.S.A.

³ To whom correspondence should be addressed.

(~ 100 kPa). The most reliable data in this range have uncertainties approaching 1 part in 10^5 of the vapor pressure, p_σ . The accuracy of most experimental vapor pressures probably falls at lower pressures by about a power of 10 for every tenfold decrease in pressure. Thus, at 1 Pa, the possible uncertainty in a vapor pressure may be about 100%. The chief objective of this work is to develop a new method to calculate reliable vapor pressures at pressure conditions where conventional measurements are frequently suspect or, in many cases, nonexistent. We first show the relevant thermodynamic equations, then review published methods, then discuss the equations specific to the new method. In the latter half of this work we apply the new method to three substances.

Procedures to extend vapor-pressure measurements to low temperatures have been based principally on thermodynamic equations for the vapor pressure. Thermodynamic equations for the vapor pressure always begin with the equality of the Gibbs energy of the coexisting phases $G'(T, p) = G''(T, p)$, which applies to vapor–solid, solid–liquid, or liquid–vapor equilibrium. For small changes in the equilibrium temperature and coexistence pressure, the changes in the Gibbs energy due to the small (dT and dp) changes must be equal, $dG' = dG''$. Substituting the Gibbs–Duhem equation for the Gibbs energy, $dG = V dp - S dT$, into this equality gives the expression, $V' dp - S' dT = V'' dp - S'' dT$. Since T and p are the same in both phases, we may rearrange this expression to obtain

$$\left(\frac{\partial p}{\partial T}\right)_\sigma = \left(\frac{S' - S''}{V' - V''}\right) = \frac{\Delta_{\text{VAP}} S}{\Delta_{\text{VAP}} V} \quad (1)$$

Substituting the definition $G = H - TS$ into the Gibbs equality we get, $H' - TS' = H'' - TS''$. Rearranging gives $S' - S'' = (H' - H'')/T$. We may substitute this last result into Eq. (1) to obtain the familiar Clapeyron equation

$$\left(\frac{\partial p}{\partial T}\right)_\sigma = \left(\frac{H' - H''}{T(V' - V'')}\right) = \frac{\Delta_{\text{VAP}} H}{T \Delta_{\text{VAP}} V} \quad (3)$$

If we then substitute the definition of $H = U + pV$, we obtain

$$\left(\frac{\partial p}{\partial T}\right)_\sigma = \left(\frac{U' - U''}{T(V' - V'')}\right) + \frac{p_\sigma}{T} = \frac{\Delta_{\text{VAP}} U}{T \Delta_{\text{VAP}} V} + \frac{p_\sigma}{T} \quad (4)$$

or we may write, more compactly,

$$T^2 \left(\frac{\partial(p/T)}{\partial T}\right)_\sigma = \frac{\Delta_{\text{VAP}} U}{\Delta_{\text{VAP}} V} \quad (5)$$

Equations (1)–(4) illustrate how we can use data for entropy, enthalpy, or internal-energy changes to extract useful information on the temperature derivatives of the saturation pressure. When combined with measurements of vapor pressure in the atmospheric range and fitted to a vapor pressure equation, we may integrate Eqs. (1)–(4) to obtain accurate vapor pressures at pressures below the atmospheric range.

Since precise experimental data for entropy, enthalpy, or internal energy for saturated liquid and vapor states are seldom available, other practical strategies have been proposed. Majer et al. [2] have extensively reviewed published work on enthalpies of vaporization. They discuss the methods for extracting vapor pressures which employ an integration of the Clapeyron equation and a knowledge of the vapor pressure at a single temperature, concluding that often there are insufficient experimental data available to obtain accurate vapor pressures. This point has been amplified by McLinden [3]. McLinden analyzed the direct integration of the Clapeyron equation for 2,2-dichloro-1,1,1-trifluoroethane (R123). McLinden used an accurate equation of state developed by Younglove and McLinden [4] to calculate all of the parameters in the Clapeyron equation, Eq. (2). To illustrate the effect of experimental uncertainties, McLinden applied a systematic +0.1% offset to the enthalpies of vaporization calculated with the equation of state, then calculated vapor pressures. Starting an integration of the Clapeyron equation at a reference state of (300 K, 97.8 kPa), he found that the calculated vapor pressure was 1% too low at 250 K, 10% too low at 215 K, and in the worst case, negative at 190 K. In practice, the experimental uncertainty of enthalpies of vaporization is often 5 to 10 times the systematic offset used by McLinden, implying that because of its sensitivity to experimental uncertainties, integration of experimental $\Delta_{\text{VAP}}H$ may be impractical over wide ranges of temperature.

Recently, however, practical approaches which may circumvent these problems have been developed. Tillner-Roth [5] has presented a method which employs a nonlinear regression analysis to extrapolate p_σ from near the normal boiling point to the triple point, based on integration of the Clapeyron equation in terms of $\ln p_\sigma$ and T^{-1} and a simple equation for $\Delta_{\text{VAP}}H$. While no experimental $\Delta_{\text{VAP}}H$ data were used, selected vapor-pressure data were employed in this method. A one-term equation for the T dependence of $\Delta_{\text{VAP}}H$ was employed which may not always adequately describe the behavior of $\Delta_{\text{VAP}}H$ over a wide range of temperatures. In any case, it has been shown to be a reliable method for refrigerants between the triple point and 0.1–0.2 MPa. The vapor pressures calculated with Tillner-Roth's method are within a few pascals (or 0.1%, whichever is greater) of experimental measurements.

Weber [6] has presented a method for extrapolating vapor-pressure data with saturated-liquid heat capacities by applying an iterative method with the equation,

$$C_{\sigma} \approx C'_{\rho} = C''_v + \frac{RT}{V''} \left(\frac{dV''}{dT} \right) - T \left(\frac{dV''}{dT} \right) \left(\frac{dp}{dT} \right)_{\sigma} - V'' T \left(\frac{d^2 p}{dT^2} \right)_{\sigma} \quad (5)$$

where C_{σ} denotes the saturated-liquid heat capacity. This is a complex method, and as with any such technique, there are possible hidden problems. For example, there is a possibility of numerical instability of the right side of Eq. (5), whose (first and second) and (third and fourth) term pairs are of nearly equal magnitude but with opposite signs. Also, knowledge of a number of complex thermodynamic properties especially the first and second derivatives, is required to evaluate the terms in this function. An ideal-gas approximation for the vapor phase is given for the second term on the right side. Weber has pointed out that the full real-gas term must be used for calculations and that Eq. (5) is better for going from p_{σ} to C_{σ} . Nevertheless, p_{σ} values estimated with this method have been successfully used to develop equations of state, for example, Refs. 4 and 7 at low temperatures.

Magee [8] has shown that useful information on the temperature derivatives of the vapor pressure may be obtained from isochoric measurements of internal-energy changes or heat capacities in the vapor + liquid coexistence region. The key measurements required are density and internal energy. In order to treat these two-phase data, the following relations will be derived beginning with the definition of the Helmholtz free energy, $A = U - TS$. Our starting point is a combination of the two expressions $U = A + TS$ and $S = -(\partial A / \partial T)_{v}$, from which we obtain

$$U = A - T(\partial A / \partial T)_{v} \quad (6)$$

The internal energy in the two-phase region, $U^{(2)}$, is a function of T and V . This is a *bulk thermophysical property*, which is a mass average of the saturated liquid and saturated vapor (specific) properties at the same T and p . We may evaluate the derivative with respect to V while T is constant,

$$(\partial U^{(2)} / \partial V)_{T} = (\partial A^{(2)} / \partial V)_{T} - T(\partial^2 A^{(2)} / \partial V \partial T) \quad (7)$$

Substituting the equality $p_{\sigma} = -(\partial A^{(2)} / \partial V)_{T}$ into Eq. (7), we obtain the expression relating the two-phase internal energy to the vapor pressure,

$$(\partial U^{(2)} / \partial V)_{T} = T \left(\frac{dp}{dT} \right)_{\sigma} - p_{\sigma} = T^2 \left(\frac{d(p/T)}{dT} \right)_{\sigma} \quad (8)$$

If we differentiate both sides of Eq. (8) with respect to T , we obtain the following result in the two-phase region:

$$(\partial C_v^{(2)}/\partial V)_T = T \left(\frac{d^2 p}{dT^2} \right)_\sigma \quad (9)$$

which could also be obtained by differentiation of an expression [their Eq. (3)] derived by Yang and Yang [9].

Equations (8) and (9) suggest a simple procedure for evaluating vapor pressure from calorimetric measurements at constant volume, such as reported by Magee [10] for 1,1,1,2-tetrafluoroethane (R134a). We can calculate discrete values of the first and second temperature derivatives of the vapor pressure for two-phase samples from internal energy measurements and the resulting heat capacity data for at least two bulk densities. These calculations will be done at temperatures which overlap existing vapor-pressure measurements near the normal boiling point and extend to much lower temperatures. Since the relationships of both internal energy to volume and heat capacity to volume must be exactly linear for two-phase states at constant temperature, only two two-phase isochores are needed for these calculations, though five or more isochores would be beneficial. The derivatives calculated with this procedure and selected measurements of vapor pressure could be fitted simultaneously to a vapor pressure equation. No assumptions have been made in the procedure. No additional corrections need be made to the raw experimental data. The recommended temperature range for this calculation and fitting procedure would be $T_{\text{TRIPLE}} < T < 0.8T_c$, since the curvature of the internal energy and heat capacity becomes very strong at temperatures close to the critical point, raising the uncertainty of the estimates of these derivatives. We demonstrate below that the procedure yields vapor pressures with a low uncertainty.

2. DETAILS OF TECHNIQUE

2.1. Working Equations

This section presents a technique for accurate evaluation of vapor pressures from isochoric internal-energy measurements in the two-phase region. For the alternative refrigerants of interest, no independent studies of $C_v^{(2)}$ measurements have been published. Since $U^{(2)}$ and $C_v^{(2)}$ from the same study would reveal much the same information, Eq. (9) was not employed in this work. The method is based solely on Eq. (8). Figure 1 illustrates the behavior of internal energy $U^{(2)}$ of a two-phase sample of

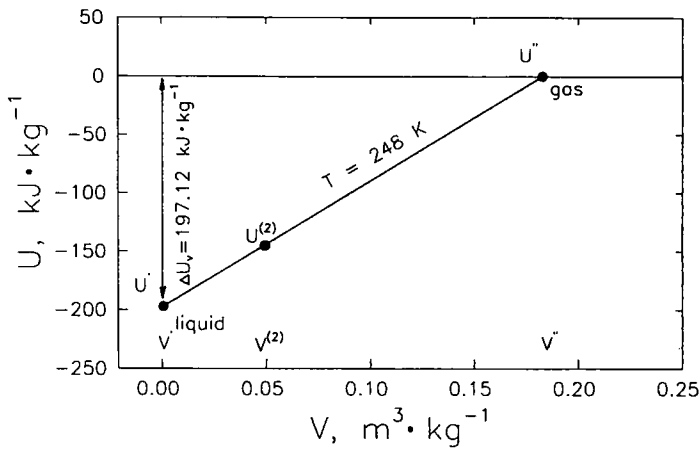


Fig. 1. Linear dependence of two-phase internal energy on bulk specific volume at a temperature near the normal boiling point of R134a; data from Ref. 11; the arbitrary reference condition is defined as $U = 0$ at the saturated vapor state at $T = 248$ K.

1,1,1,2-tetrafluoroethane (R134a) at a constant temperature of 248 K. This temperature is slightly higher than the normal boiling point [11] of 246.78 K. The internal-energy function in Fig. 1 varies linearly from the saturated liquid U' to the saturated vapor U'' , to which we have assigned an arbitrary value of 0. At a bulk two-phase specific volume $V^{(2)}$, the bulk internal energy is $U^{(2)}$. Since $U^{(2)}$ is a linear function of $V^{(2)}$ at any given temperature, $(\partial U^{(2)}/\partial V^{(2)})_T$ is a unique value that can be determined easily with finite differences by any two $(U^{(2)}, V^{(2)})$ pairs of values within the two-phase region. This derivative is evaluated with the expression,

$$(\partial U^{(2)}/\partial V^{(2)})_T = \left(\frac{U_2^{(2)} - U_1^{(2)}}{V_2^{(2)} - V_1^{(2)}} \right)_T \quad (10)$$

where the subscripts 1 and 2 denote any two points within the two-phase region, including the points at the saturated single phases and the superscript (2) denotes the bulk property (that is, the property of the vapor and the liquid combined).

After computing $(\partial U^{(2)}/\partial V^{(2)})_T$ at different temperatures in the temperature range of interest, we can fit these values to Eq. (8), [with an appropriate model for $p_\sigma(T)$] to produce vapor pressures using nonlinear regression [12]. The regression analysis must fit the adjustable parameters in the difference between two equations: those for $T(dp/dT)_\sigma$ and p_σ . In order to be successful, we must select a model for $p_\sigma(T)$ which is capable

of fitting vapor-pressure data within experimental uncertainty over the entire temperature range of interest.

The best source of experimental values for $U^{(2)}$ is from isochoric (constant $V^{(2)}$) measurements with an adiabatic calorimeter. At least two isochores are needed to calculate the change of the bulk internal energy with respect to the bulk specific volume at constant temperature. Since the calorimetric measurements provide the change of internal energy along a given isochore, but not the change of internal energy from one isochore to another, we need additional information at a reference temperature to determine the change of internal energy between two isochores. This reference temperature is selected near the normal boiling point, where accurate, direct measurements of vapor pressure are available.

$(\partial U^{(2)}/\partial V^{(2)})_T$ at the reference temperature can be calculated with Eq. (8) and vapor-pressure data around the reference temperature. Then the change of internal energy from isochore 1 to isochore 2 at that reference temperature can be determined as follows:

$$U_2^{(2)} - U_1^{(2)} = (\partial U^{(2)}/\partial V^{(2)})_T (V_2^{(2)} - V_1^{(2)}) \quad (11)$$

In this procedure, we set the internal energy of one of the isochores ($U_2^{(2)}$ or $U_1^{(2)}$) to an arbitrary value at the reference temperature.

2.2. Test of Technique with Equation-of-State Calculations

We tested this procedure with $(\partial U/\partial V)_T$ values generated with an equation of state for the temperature range of interest. We calculated internal energies for R134a in the single-phase fluid at the saturated liquid and vapor densities with the Tillner-Roth [11] equation of state and compared the vapor-pressure values produced by the technique presented in this work with the Huber and McLinden [7] vapor-pressure equation for R134a. At 248 K, the vapor pressure produced with the $(\partial U/\partial V)_T$ values is 13 Pa lower (-0.01%) than the value from the vapor-pressure equation. At 210.0 K, it is 14 Pa higher ($+0.1\%$). At the triple-point temperature (169.85 K), it is 3 Pa higher ($+0.8\%$). We have demonstrated that there is good consistency between the equation of state developed by Tillner-Roth and Baehr and the vapor-pressure equation independently determined by Huber and McLinden. More importantly, these results demonstrate the effectiveness of the working equations and methodology developed for this project.

2.3. Application to Three Substances

This method was applied to three alternative refrigerants: 1,1,1,2-tetrafluoroethane (R134a), pentafluoroethane (R125), and difluoromethane

(R32). These fluids were chosen because of the availability of calorimetric data. Magee and co-workers [10, 14] measured $\Delta U^{(2)}$ and $V^{(2)}$ along two-phase isochores with an adiabatic calorimeter. Initially, we used Magee's [10] calorimetric data from the isochores with the highest and lowest densities. The difference in internal energy between the two isochores is about $15 \text{ J} \cdot \text{mol}^{-1}$ at the reference temperature and about $0.2 \text{ J} \cdot \text{mol}^{-1}$ at the triple-point temperature. With an uncertainty of $0.1 \text{ J} \cdot \text{mol}^{-1} \cdot \text{K}^{-1}$ for $\Delta U^{(2)}/\Delta T$, it was not possible to determine $(\partial U^{(2)}/\partial V^{(2)})_T$ with sufficient accuracy. Unfortunately, the published two-phase isochores are too close to the saturated liquid and too close among themselves.

The normal boiling-point and triple-point temperatures for R134a are 246.78 K [11] and 169.85 K [10], respectively. A temperature of 248 K was selected for the reference temperature due to the availability of tabulated saturation curve data. The internal-energy reference state, where we arbitrarily set $U=0$, was selected as the saturated vapor at 248 K . We have evaluated vapor pressures for R134a from 248 K to the triple-point temperature.

Experimental data on internal-energy changes at a low ($0.01 < \rho/\rho_c < 0.1$) bulk density have not been published for R134a. As a substitute, we used internal energies of the saturated vapor from an equation of state for our low-density states. We paired this with a high-density isochore from calorimetric measurements. The difference in internal energy between these two curves is about $20 \text{ kJ} \cdot \text{mol}^{-1}$ at the reference temperature and about $25.5 \text{ kJ} \cdot \text{mol}^{-1}$ at the triple-point temperature. The large absolute values we obtained for $\Delta U^{(2)}$ allow us to calculate accurate values of $(\partial U^{(2)}/\partial V^{(2)})_T$.

In order to determine the magnitude of the real-gas contribution, we obtained the saturated-vapor internal energies in two ways. First, looking at only the ideal-gas contribution, we employed ideal-gas heat capacities [11] for the determination of internal energies. The ancillary equation reported by Tillner-Roth [11] was employed for saturated-vapor densities. With this approach, we obtained estimated vapor pressures which were slightly high. A comparison with the vapor-pressure equation reported by Huber and McLinden [7] and the vapor-pressure equation reported by Tillner-Roth [11] shows a deviation of $+160 \text{ Pa}$ ($+0.2\%$) at the reference temperature and $+20 \text{ Pa}$ ($+5\%$) at the triple point.

In the second case, we included the volumetric contribution to internal energies from $dU = C_v dT + (\partial U/\partial V)_T dV$ by using the Tillner-Roth [11] equation of state for the gas-phase properties of R134a. This led to excellent results for the calculated vapor pressures. A comparison with the vapor-pressure equation reported by Huber and McLinden [7] shows a deviation of -32 Pa (-0.03%) at the reference temperature and -3 Pa (-0.8%) at the triple point.

Our primary focus is the development of a new equation of state for a fluid of interest. For this task, reliable vapor pressures are essential input data for the fitting procedure. These data should ideally cover a broad range of temperatures. In most cases, there are ample p_σ data near ambient conditions, but data are scarce at very low temperatures. In these cases, we use the ideal-gas calculation in the first iteration, then fit a preliminary version of an equation of state and use it to calculate the volumetric contribution. We iterate this process until the results converge.

In order to test the sensitivity of this procedure to the form of the vapor-pressure equation, we used two functions for the vapor pressure $p_\sigma(T)$ model in Eq. (8): the first is an equation of Huber and McLinden [7],

$$\ln \frac{p_\sigma}{p_c} = C_1 \tau^\varepsilon + C_2 \left(\frac{\tau}{1-\tau} \right) + C_3 \tau + C_4 \tau^3 \tag{12}$$

where $\tau = 1 - T/T_c$, $\varepsilon = 1.66$, $T_c = 374.179$ K, and $p_c = 4.056$ MPa.

The second equation is from Tillner-Roth [11]:

$$\ln \frac{p_\sigma}{p_c} = \frac{1}{T_r} [C_1 \tau + C_2 \tau^{1.5} + C_3 \tau^2 + C_4 \tau^4] \tag{13}$$

where $T_c = 374.18$ K and $p_c = 4.05629$ MPa.

We obtained nearly identical (± 2 Pa) vapor-pressure results when the calculated data are fitted to either Eq. (12) or Eq. (13). Thus, the technique is independent of the model used for $p_\sigma(T)$, as long as this model is capable of fitting experimental vapor pressures in the temperature range of interest. Table I presents the fitting parameters (C_1 , C_2 , C_3 , and C_4) from experimental vapor pressures for both vapor-pressure equations.

Table I. Parameters for Vapor-Pressure Ancillary Equations

	C_1	C_2	C_3	C_4	C_5
Eq. (12), R134a ^a	3.946984	-11.313271	3.693108	5.566337	--
Eq. (13), R134a ^b	-7.686556	2.311791	-2.039554	-3.583758	--
Eq. (17), R125 ^c	-7.435645	1.341794	-3.367536	-1.697153	--
Eq. (18), R32 ^c	-7.559554	2.465252	-1.976887	-2.021284	-1.941251
Eq. (12), R134a	4.023776	-11.382390	3.746555	5.675758	--
Eq. (17), R125	-7.517629	1.530640	-3.618286	-1.802400	--
Eq. (18), R32	-7.566935	2.484133	-1.984020	-2.067412	-1.921275

^a From Ref. 7.

^b From Ref. 11.

^c From Ref. 13.

Table II. Intermediate Values for the Calculation of $(\partial U/\partial V)_T$ and Comparison of the Internal Energy of Vaporization $\Delta_{\text{VAP}}U$ for R134a

T (K)	J'' ($\text{m}^3 \cdot \text{kg}^{-1}$)	$J'^{2,1}$ ($\text{m}^3 \cdot \text{kg}^{-1}$)	U'' ($\text{kJ} \cdot \text{kg}^{-1}$)	$U'^{2,1}$ ($\text{kJ} \cdot \text{kg}^{-1}$)	$U'' - U'^{2,1}$ ($\text{kJ} \cdot \text{kg}^{-1}$)	$(\partial U/\partial V)_T$ (MPa)	$\Delta_{\text{VAP}}U$ ($\text{kJ} \cdot \text{kg}^{-1}$)	$\Delta_{\text{VAP}}U_{\text{calc}}$ ($\text{kJ} \cdot \text{kg}^{-1}$) ^a	Diff. (%) ^b
248	0.182792	0.00073944	0.00	-197.05	197.05	1.08239710	197.07	197.12	0.03
246	0.199263	0.00073937	-1.15	-199.60	198.45	0.99964756	198.47	198.52	0.03
244	0.217557	0.00073931	-2.29	-202.14	199.85	0.92174011	199.87	199.93	0.03
242	0.237925	0.00073925	-3.45	-204.68	201.23	0.84841120	201.25	201.32	0.04
240	0.260641	0.00073919	-4.59	-207.21	202.61	0.77957022	202.63	202.71	0.04
238	0.286025	0.00073912	-5.74	-209.73	203.99	0.71502692	204.01	204.09	0.04
236	0.314456	0.00073906	-6.90	-212.24	205.35	0.65456218	205.37	205.46	0.05
234	0.346356	0.00073900	-8.04	-214.75	206.71	0.59810334	206.73	206.82	0.04
232	0.382234	0.00073893	-9.18	-217.25	208.07	0.54541111	208.09	208.18	0.04
230	0.422672	0.00073887	-10.33	-219.75	209.42	0.49633464	209.44	209.54	0.05
228	0.468362	0.00073880	-11.47	-222.24	210.77	0.45072547	210.79	210.89	0.05
226	0.520102	0.00073874	-12.61	-224.72	212.11	0.40840173	212.13	212.23	0.05
224	0.578871	0.00073868	-13.75	-227.20	213.45	0.36920315	213.47	213.58	0.05
222	0.645745	0.00073861	-14.89	-229.67	214.78	0.33299324	214.80	214.91	0.05
220	0.722022	0.00073855	-16.02	-232.14	216.12	0.29962742	216.13	216.26	0.06
218	0.809389	0.00073848	-17.16	-234.60	217.44	0.26888919	217.45	217.58	0.06
216	0.909587	0.00073842	-18.29	-237.05	218.76	0.24070431	218.78	218.91	0.06
214	1.024821	0.00073835	-19.42	-239.50	220.08	0.21490261	220.09	220.22	0.06
212	1.157890	0.00073829	-20.53	-241.94	221.41	0.19133900	221.42	221.56	0.06
210	1.311957	0.00073822	-21.65	-244.38	222.73	0.16986169	222.74	222.88	0.06

208	1.490868	0.00073816	-22.76	-246.81	224.05	0.15035379	224.06	224.2	0.06
206	1.699351	0.00073810	-23.87	-249.23	225.36	0.13267446	225.37	225.52	0.07
204	1.943068	0.00073803	-24.98	-251.65	226.67	0.11670135	226.68	226.84	0.07
202	2.228959	0.00073797	-26.07	-254.07	228.00	0.10232193	228.00	228.17	0.07
200	2.565616	0.00073791	-27.17	-256.48	229.31	0.08940193	229.31	229.48	0.07
198	2.963402	0.00073784	-28.25	-258.88	230.63	0.07784455	230.63	230.80	0.07
196	3.435246	0.00073778	-29.37	-261.28	231.91	0.06752487	231.92	232.10	0.08
194	3.997282	0.00073772	-30.44	-263.68	233.24	0.05835962	233.24	233.42	0.08
192	4.669406	0.00073766	-31.51	-266.07	234.56	0.05024180	234.57	234.74	0.08
190	5.476751	0.00073760	-32.59	-268.46	235.87	0.04307364	235.88	236.06	0.08
188	6.450365	0.00073754	-33.64	-270.84	237.20	0.03677782	237.21	237.39	0.08
186	7.630093	0.00073748	-34.67	-273.22	238.55	0.03126791	238.56	238.75	0.08
184	9.066183	0.00073742	-35.73	-275.60	239.87	0.02645984	239.87	240.07	0.08
182	10.82368	0.00073737	-36.79	-277.98	241.19	0.02228469	241.19	241.38	0.08
180	12.98533	0.00073731	-37.83	-280.35	242.52	0.01867779	242.53	242.73	0.08
178	15.65435	0.00073726	-38.74	-282.72	243.98	0.01558587	243.98	244.18	0.08
176	18.97533	0.00073721	-39.75	-285.09	245.33	0.01292962	245.34	245.54	0.08
174	23.12139	0.00073715	-40.90	-287.46	246.56	0.01066402	246.56	246.77	0.08
172	28.33664	0.00073711	-41.74	-289.92	248.08	0.00875513	248.09	248.30	0.08
170	34.94060	0.00073706	-42.99	-292.19	249.20	0.00713222	249.20	249.41	0.09
169.85	35.49876	0.00073705	-42.94	-292.37	249.43	0.00702654	249.43	249.64	0.09

^a From Ref. 11.

^b $100 * (\Delta_{VAP} U_{c,calc} - \Delta_{VAP} U) / \Delta_{VAP} U_{c,calc}$.

In every test case presented for R134a, the change in internal energy along the high-density isochore was determined from Magee's [10] two-phase calorimetric data. We chose an isochore that includes measurements from 175.830 to 250.426 K. For this isochore, the calorimetric bomb (with a volume of approximately 73 cm³) contained 0.9697 mol of sample. The energy needed to change the temperature of the sample by 1 K was fitted to the equation

$$Q/\Delta T = a_0 + a_1 T^{-1} + a_2 T^{-2} \quad (14)$$

where Q is in J and T is in K. The coefficients are $a_0 = 2.10249278 \times 10^2$, $a_1 = -3.17356599 \times 10^4$, and $a_2 = 2.70115464 \times 10^6$.

The change of internal energy along the isochore is then calculated as

$$\Delta U = \frac{\int_{T_1}^{T_2} (Q/\Delta T) dT}{n} \quad (15)$$

where $n = 0.9697$ mol.

The density of the isochore was fitted to the equation (the exact bomb volume varies with temperature and pressure)

$$\rho = b_0 + b_1 T^{-1} + b_2 T^{-2} \quad (16)$$

where ρ is in mol · dm⁻³ and the coefficients are $b_0 = 1.30197341 \times 10^1$, $b_1 = 8.23883179 \times 10^1$, and $b_2 = -5.97789093 \times 10^3$. The molecular weight used for R134a is 102.03 g · mol⁻¹.

The internal energy and density of the saturated vapor were calculated with the Tillner-Roth [11] equation of state for R134a. Any other gas-phase equation of state which reproduces the correct behavior of the second virial coefficients could have served the same purpose. A value of $(\partial U^{(2)}/\partial V^{(2)})_T$ at the reference temperature (248 K) was calculated with the vapor-pressure ancillary equation of Huber and McLinden [7]. To show the contribution of each term in Eq. (10), intermediate values of the specific volume, internal energy, and $(\partial U^{(2)}/\partial V^{(2)})_T$ are presented in Table II. In addition, we have shown that the internal energies of vaporization $\Delta_{\text{VAP}}U$ are only slightly higher (< 0.02 kJ · kg⁻¹) than the two-phase ΔU values used to determine vapor pressures. Thus, most of the internal energy change needed to span the two-phase region has been employed to evaluate vapor pressures with this technique. The $\Delta_{\text{VAP}}U$ values were shown to be within 0.09% of those given by Tillner-Roth and Baehr [11]. This result implies that our vapor pressures will be thermodynamically consistent with the Tillner-Roth and Baehr equation of state.

For R125, we used the vapor pressure ancillary equation of Outcalt and McLinden [13] as our model for $p_\sigma(T)$ in Eq. (8)

$$\ln \frac{p_\sigma}{p_c} = \frac{C_1 \tau + C_2 \tau^{1.5} + C_3 \tau^3 + C_4 \tau^6}{1 - \tau} \quad (17)$$

where $\tau = 1 - T/T_c$, $T_c = 339.33$ K, and $p_c = 3.629$ MPa. The fitting parameters of Outcalt and McLinden [13] obtained from experimental vapor-pressure data are shown in Table I.

An isochore with a total of 0.86966 mol was chosen from the calorimetric data measured by Lüddecke and Magee [14]. The change of internal energy along the two-phase isochore was calculated with Eqs. (14) and (15). The fitting parameters for Eq. (14) are $a_0 = 1.99691908 \times 10^2$, $a_1 = -2.81467285 \times 10^4$, and $a_2 = 2.11451248 \times 10^6$. The density of the isochore was fitted to Eq. (16) within experimental uncertainty. The fitting parameters for this equation are $b_0 = 1.16836327 \times 10^1$, $b_1 = 7.52740868 \times 10^1$, and $b_2 = -5.51047455 \times 10^3$. For R125, $M = 120.02$ g·mol⁻¹. The internal energy and density of the saturated vapor were calculated with the equation of state for R125 of Outcalt and McLinden [13]. $(\partial U/\partial V)_T$ at the reference temperature (225.15 K) was calculated with the vapor-pressure ancillary equation of Outcalt and McLinden [13].

For R32, we used the vapor-pressure ancillary equation of Outcalt and McLinden [13] as our model for $p_\sigma(T)$ in Eq. (8),

$$\ln \frac{p_\sigma}{p_c} = \frac{C_1 \tau + C_2 \tau^{1.5} + C_3 \tau^2 + C_4 \tau^6 + C_5 \tau^{6.5}}{1 - \tau} \quad (18)$$

where $T_c = 351.35$ K and $p_c = 5.795$ MPa. The fitting parameters of Outcalt and McLinden [13] obtained from experimental vapor pressure data are shown in Table I.

An isochore with a total of 1.28723 mol was chosen from the calorimetric data measured by Lüddecke and Magee [14]. The change in internal energy along the two-phase isochore was calculated with Eqs. (14) and (15). The fitting parameters for Eq. (14) are $a_0 = 1.48365613 \times 10^2$, $a_1 = -1.51249056 \times 10^4$, and $a_2 = 1.30273164 \times 10^6$. The density of the isochore was fitted to Eq. (16) within experimental uncertainty. The fitting parameters for this equation are $b_0 = 1.73805482 \times 10^1$, $b_1 = 7.8201792 \times 10^1$, and $b_2 = -4.86941367 \times 10^3$. For R32, $M = 52.024$ g·mol⁻¹. The internal energy and density of the saturated vapor were calculated with the Outcalt and McLinden [13] equation of state for R32. $(\partial U/\partial V)_T$ at the reference temperature (221.15 K) was calculated with the vapor pressure ancillary equation of Outcalt and McLinden [13].

3. RESULTS

3.1. Vapor Pressures for R134a, R125, and R32

We have devised a technique to evaluate accurate vapor pressures from calorimetric data. We calculated vapor pressures from the triple-point temperature to around the normal boiling-point temperature for the following fluids: R134a, R125, and R32. Tables III, IV, and V present vapor pressures for R134a, R125, and R32, respectively. The bottom of Table I presents the fitting parameters (obtained with the present technique) for the vapor pressure equations. Deviations of these vapor pressures from the respective vapor-pressure ancillary equations are shown in Figs. 2, 3, and 4. The figures also show how some accurate vapor pressure data deviate from the vapor pressure equations.

Figure 2 (R134a) shows excellent agreement between the vapor pressures determined by this technique and vapor pressures measured by Magee and Howley [15]. It also shows agreement within experimental uncertainty of 20–40 Pa (0.02–0.04%) for vapor pressures by Goodwin et al. [16].

For R125, Fig. 3 shows that the vapor pressures determined in this work are systematically lower than the vapor pressure from the ancillary equation. This is not necessarily a bad result, because they fall precisely between two published data sets. The vapor pressures are just below (-30 Pa, -0.03%) the vapor pressures by Magee [17] around the normal boiling point and are just above ($+30$ Pa, $+0.03\%$) the data of Weber and Silva [18], also around the normal boiling-point temperature. At the triple-point temperature there is good agreement (± 30 Pa, $\pm 1\%$) with the values calculated from C_σ measurements reported by Lüddecke and Magee [14] and also the values Weber and Silva calculated using the same C_σ data.

Figure 4 shows vapor-pressure deviations for R32. Our calculated vapor pressures agree (within experimental uncertainty, ± 40 Pa, $\pm 0.04\%$) with the vapor pressures measured by Weber and Goodwin [19] around the normal boiling-point temperature. At the triple-point temperature, there is good agreement (< 5 Pa) between our values and values calculated from C_σ measurements [14].

3.2. Estimation of Uncertainties

This section presents the sources of uncertainty for the calculated vapor pressures. This includes the effect of the model used for $p_\sigma(T)$, the effect of the vapor-pressure data used to calculate $(\partial U/\partial V)_T$ at the reference

Table III. Vapor Pressures Derived from $U^{(2)}$ and from Published Data for R134a

T (K)	p_{σ} (Pa)	$p_{\sigma, \text{published}}$ (Pa) ^a	$p_{\sigma} - p_{\sigma, \text{published}}$ (Pa)
169.85	390.2	393.4	-3.1
170.00	396.8	400.0	-3.2
175.00	681.2	685.8	-4.6
180.00	1,128.4	1,134.8	-6.4
185.00	1,809.6	1,818.3	-8.6
190.00	2,817.5	2,828.7	-11.2
195.00	4,269.6	4,283.6	-14.0
200.00	6,311.4	6,328.5	-17.1
205.00	9,119.6	9,139.7	-20.1
210.00	12,903.9	12,926.9	-23.0
215.00	17,909.7	17,935.3	-25.6
220.00	24,418.8	24,446.6	-27.8
225.00	32,750.6	32,780.1	-29.4
230.00	43,262.6	43,293.2	-30.6
235.00	56,349.6	56,380.9	-31.2
240.00	72,443.7	72,475.4	-31.7
245.00	92,013.0	92,045.3	-32.3
250.00	115,560.3	115,593.7	-33.5

^a From Ref. 7.Table IV. Vapor Pressures Derived from $U^{(2)}$ and from Published Data for R125

T (K)	p_{σ} (Pa)	$p_{\sigma, \text{published}}$ (Pa) ^a	$p_{\sigma} - p_{\sigma, \text{published}}$ (Pa)
172.52	2,915.6	2,953.1	-37.4
175.00	3,653.7	3,695.8	-42.0
180.00	5,630.7	5,682.1	-51.4
185.00	8,439.2	8,499.5	-60.4
190.00	12,331.8	12,399.9	-68.1
195.00	17,607.1	17,680.9	-73.8
200.00	24,611.4	24,688.3	-76.9
205.00	33,739.4	33,816.5	-77.1
210.00	45,434.1	45,508.8	-74.7
215.00	60,185.2	60,255.9	-70.7
220.00	78,528.0	78,594.9	-67.0
225.00	101,040.6	101,106.8	-66.2

^a From Ref. 13.

Table V. Vapor Pressures Derived from $U^{(2)}$ and from Published Data for R32

T (K)	p_{σ} (Pa)	$p_{\sigma, \text{published}}$ (Pa) ^a	$p_{\sigma} - p_{\sigma, \text{published}}$ (Pa)
136.34	46.5	46.9	-0.5
140.00	81.4	82.1	-0.7
145.00	166.1	167.4	-1.3
150.00	320.6	322.7	-2.1
155.00	589.1	592.4	-3.4
160.00	1,035.3	1,040.4	-5.1
165.00	1,748.5	1,755.8	-7.3
170.00	2,848.6	2,858.7	-10.1
175.00	4,492.0	4,505.5	-13.4
180.00	6,877.6	6,894.9	-17.3
185.00	10,251.1	10,272.6	-21.5
190.00	14,910.3	14,936.3	-26.0
195.00	21,208.4	21,238.9	-30.5
200.00	29,556.9	29,591.6	-34.8
205.00	40,427.7	40,466.3	-38.6
210.00	54,354.2	54,396.1	-41.9
215.00	71,931.5	71,975.9	-44.4
220.00	93,815.5	93,861.6	-46.1

^a From Ref. 13.

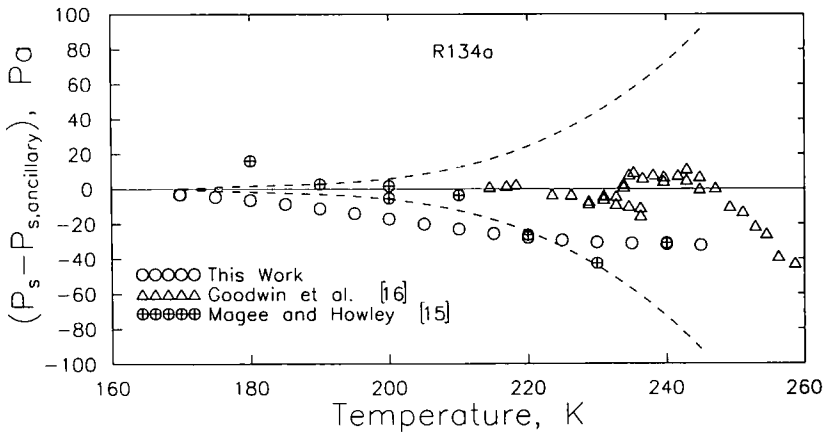


Fig. 2. Comparison of vapor pressures for R134a calculated with the present method and selected experimental values with the ancillary vapor-pressure equation of Huber and McLinden [7]; dashed lines are $\pm 0.1\%$ deviations.

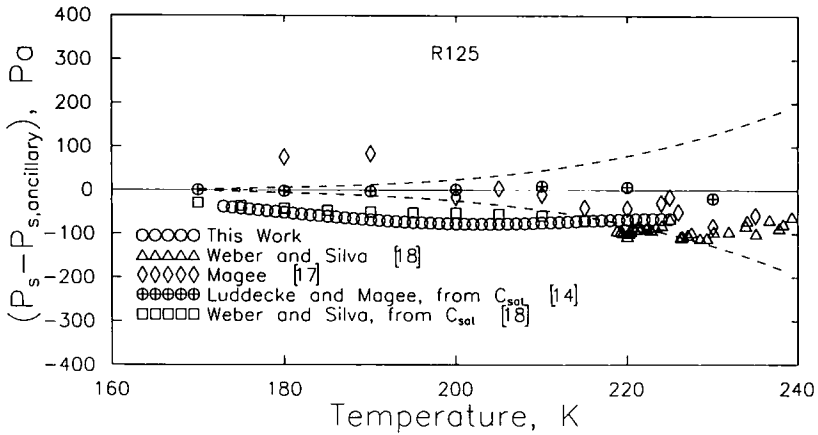


Fig. 3. Comparison of vapor pressures for R125 calculated with the present method and selected experimental values with the ancillary vapor-pressure equation of Outcalt and McLinden [13]; dashed lines are $\pm 0.1\%$ deviations.

temperature, the effect of an uncertainty in the saturated vapor specific volume (V''), the isochoric heat capacity of the ideal gas (C_v^{IG}), the specific volume of the high-density isochore ($V^{(2)}$), and the change of internal energy along the high-density isochore ($\Delta U^{(2)}/\Delta T$). The uncertainties we quote correspond to a coverage factor of 2 and were calculated using the properties of R134a. Tables II and III and published tables in Refs. 7 and

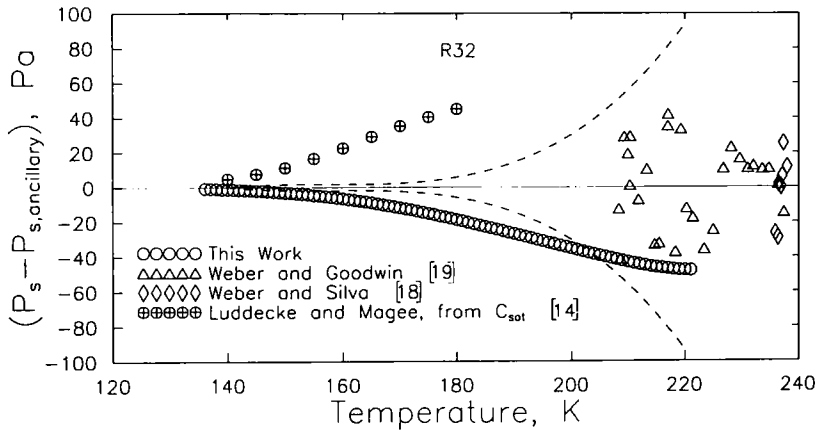


Fig. 4. Comparison of vapor pressures for R32 calculated with the present method and selected experimental values with the ancillary vapor-pressure equation of Outcalt and McLinden [13]; dashed lines are $\pm 0.1\%$ deviations.

11 may serve as guides to the intermediate values used in the calculations. We present comparisons of the vapor pressures at the triple-point temperature, a middle temperature (210 K), and a temperature near the normal boiling-point temperature (245 K). The vapor pressures are 390, 12,904, and 92,013 Pa at these temperatures. An estimate of the overall uncertainty in the evaluated vapor pressures is presented.

We evaluated the vapor pressure of R134a by fitting to two equations representing $p_{\sigma}(T)$ in Eq. (8). We used both Eq. (12) and Eq. (13) in this technique. Practically the same values are obtained from both equations. Differences between the vapor pressures are 4.2 Pa (0.004%) at 245 K, 2.4 Pa at 210 K, and 2.5 Pa at the triple point. This implies that the results of this technique are only weakly dependent on the model used to determine $p_{\sigma}(T)$, as long as the model is capable of representing data over a wide range of temperature.

In this technique, we need to evaluate $(\partial U/\partial V)_T$ from vapor-pressure data at a reference temperature. Two vapor-pressure equations from Huber and McLinden [7] and Tillner-Roth and Baehr [11] were employed. The difference between the calculated vapor pressures is 25.1 Pa (0.025%) at 245 K, 3.4 Pa at 210 K, and 0.1 Pa at the triple-point temperature. We get close to the same results whether we choose one or the other ancillary equation for the reference calculation. It is also apparent that the effect of an error in the $(\partial U/\partial V)_T$ value assigned to the reference temperature diminishes as the temperature decreases.

We applied a systematic offset of $\pm 0.5\%$ to the specific volumes of the saturated vapor to test the sensitivity of this method to this quantity. Uncertainty in the density translates directly into uncertainty in the calculation of U'' . This offset represents the largest estimated uncertainty for these specific volumes. This offset causes a difference in the evaluated vapor pressures of ± 30.0 Pa (0.03%) at 245.0 K, ± 8.5 Pa at the middle temperature, and ± 0.2 Pa at the triple-point temperature. These differences will be incorporated into the propagation of uncertainties.

For this fluid, the uncertainty in the isochoric heat capacity of the ideal gas ($C_v^{(i)}$) is estimated to be $\pm 0.5\%$. This amounts to an uncertainty in U'' of about $0.3 \text{ J} \cdot \text{mol}^{-1}$. Since the ideal-gas contribution is the principal part of $U''(T)$ at low pressures, this is the principal source of uncertainty for the evaluation of the internal energy of the saturated vapor. This offset causes a difference in the evaluated vapor pressures of ± 27.0 Pa (0.03%) at 245 K, ± 7.0 Pa at 210 K, and ± 0.2 Pa at the triple-point temperature.

Because the specific volume of the high-density isochore is negligible compared to the specific volume of the saturated vapor even large uncertainties in this quantity do not significantly affect the evaluated vapor

pressures. The specific volumes of the high-density isochore are estimated to have uncertainties less than $\pm 0.2\%$. This quantity does not have a significant effect in the evaluation of vapor pressures.

For this fluid, the uncertainty of $(\Delta U^{(2)}/\Delta T)$ is estimated to be $0.1 \text{ J} \cdot \text{mol}^{-1} \cdot \text{K}^{-1}$ (0.1%). An uncertainty of $\pm 0.1\%$ in $(\Delta U^{(2)}/\Delta T)$ causes a difference in the evaluated vapor pressures of $\pm 9.0 \text{ Pa}$ (0.009%) at 245 K, $\pm 3.0 \text{ Pa}$ at 210 K, and $\pm 0.1 \text{ Pa}$ at the triple-point temperature.

Using the square root of the sum of squares method, we estimated the combined uncertainty of our vapor pressure values as $\pm 48.0 \text{ Pa}$ (+0.05%) at 245 K, $\pm 12.0 \text{ Pa}$ ($\pm 0.09\%$) at 210 K, and $\pm 2.5 \text{ Pa}$ ($\pm 0.6\%$) at the triple-point temperature.

3.3. Vapor-Pressure Extrapolation or Evaluation

In addition to fitting $(\partial U/\partial V)_T$ vs T for R134a, we added experimental vapor pressures at temperatures close to the reference temperature (248 K) and fitted them simultaneously to the same $p_\sigma(T)$ equation. We had 39 $(\partial U/\partial V)_T$ points and 31 vapor-pressure points. The $(\partial U/\partial V)_T$ data range from the reference temperature to the triple-point temperature, while the vapor-pressure data range from 245 to 260 K. The effect of including the experimental vapor pressure data is negligible. The evaluated vapor pressure was only 4 Pa (0.004%) higher at 245 K, was only 2 Pa higher at 210 K, and remained the same at the triple-point temperature. This emphasizes the fact that *this technique is not an extrapolation of existing vapor pressures but it is an evaluation of the vapor pressure from calorimetric data.*

4. CONCLUSIONS

A novel method was presented for evaluation of vapor pressures from measured internal-energy changes and reference values of the vapor pressure and its derivative with temperature evaluated near the normal boiling-point temperature. In this application, internal-energy changes of the saturated vapor calculated from an equation of state or from the ideal-gas heat capacity were substituted for experimental measurements of ΔU at low densities without incurring higher uncertainties. Alternatively, this technique can employ calorimetric data to verify the thermodynamic consistency of vapor-pressure data and correlations of such data. Agreement of our calculated vapor pressures for R134a with accurate ($\pm 0.02\text{-kPa}$) measurements by Goodwin et al. [16] was within $\pm 0.04 \text{ kPa}$ ($\pm 0.04\%$), near the normal boiling point) at temperatures between 214 and 248 K. Consistency with the equation of state of Tillner-Roth and Baehr was

demonstrated by the agreement of internal energies of vaporization with the calculated values within $0.2 \text{ kJ} \cdot \text{kg}^{-1}$ (0.09%). A propagation-of-uncertainties analysis was used to estimate the uncertainty of the vapor pressures determined with this method. When applied to R134a, we estimated the uncertainty (coverage factor of 2) of the vapor pressure to be 0.05% at 245 K, 0.09% at 210 K, and 0.6% at 169.85 K. These uncertainties are of the same order of magnitude as those from carefully designed experiments for direct measurements of vapor pressures.

ACKNOWLEDGMENTS

We are especially grateful to Mark McLinden, Marcia Huber, Torsten Lüddecke, Lloyd Weber, and Reiner Tillner-Roth for many beneficial discussions during this study. We gratefully acknowledge the National Science Foundation for their support of H. A. Duarte-Garza during his stay at NIST. This material is based on activities supported by the National Science Foundation under Agreement 9527385. Any opinions, findings, and conclusions or recommendations expressed in this publication are those of the authors and do not necessarily reflect the views of the National Science Foundation. The calorimetric measurements utilized in this work were supported in part by the Air Conditioning and Refrigeration Technology Institute.

NOMENCLATURE

C_{σ}	Saturated liquid heat capacity
C_v^{ID}	Isochoric heat capacity of the ideal gas
M	Molecular weight
p_{σ}	Vapor pressure
$Q/\Delta T$	Amount of energy needed to change the temperature of the sample by 1 K
ρ	Density
T	Temperature
τ	$1 - T/T_c$

Superscript Notation

'	Saturated liquid
"	Saturated vapor
(2)	$\equiv \{m_l X' + m_g X''\} / \{m_l + m_g\}$, bulk property $X^{(2)}$ in the two-phase region for a specific property X , where m_l and m_g are, respectively, the masses of the liquid and gas

Subscript Notation

Δ_{VAP}	Change due to vaporization
v	Constant volume (isochoric)
T	Constant temperature (isothermal)
C	Critical property
σ	Saturation property

REFERENCES

1. D. Ambrose and R. H. Davies, *J. Chem. Thermodynam.* **12**:871 (1980).
2. V. Majer, V. Svoboda, and J. Piek, *Heats of Vaporization of Fluids* (Elsevier, New York, 1989).
3. M. O. McLinden, private communication (NIST, Boulder, CO, 1995).
4. B. A. Younglove and M. O. McLinden, *J. Phys. Chem. Ref. Data* **23**:731 (1994).
5. R. Tillner-Roth, *Int. J. Thermophys.* (1996), in press.
6. L. A. Weber, *Int. J. Refrig.* **17**:117 (1992).
7. M. L. Huber and M. O. McLinden, *Proc. Int. Refrig. Conf.*, Purdue University, Lafayette, IN (1992), p. 453.
8. J. W. Magee, *J. Res. Natl. Inst. Stand. Technol.* **96**:725 (1991).
9. C. N. Yang and C. P. Yang, *Phys. Rev. Lett.* **13**:303 (1964).
10. J. W. Magee, *Int. J. Refrig.* **15**:372 (1992).
11. R. Tillner-Roth and H. D. Baehr, *J. Phys. Chem. Ref. Data* **23**:657 (1994).
12. P. T. Boggs, R. H. Byrd, J. E. Rogers, and R. B. Schnabel, *NISTIR 4834 User's Reference Guide for ODRPACK Version 2.01, Software for Weighted Orthogonal Distance Regression* (NIST, Gaithersburg, MD, 1992).
13. S. L. Outcalt and M. O. McLinden, *Int. J. Thermophys.* **16**:79 (1995).
14. T. O. Lüddecke and J. W. Magee, *Int. J. Thermophys.* **17**:823 (1996).
15. J. W. Magee and J. B. Howley, *Int. J. Refrig.* **15**:362 (1992).
16. A. R. H. Goodwin, D. R. Defibaugh, and L. A. Weber, *Int. J. Thermophys.* **13**:837 (1992).
17. J. W. Magee, *Int. J. Thermophys.* **17**:803 (1996).
18. L. A. Weber and A. M. Silva, *J. Chem. Eng. Data* **39**:808 (1994).
19. L. A. Weber and A. R. H. Goodwin, *J. Chem. Eng. Data* **38**:254 (1993).